Measurement of Ion Energy Distribution Function of Fast Plasma Flow Driven by Plasma Focus Device Using Retarding Field Energy Analyzer*)

Takuya OGUCHI, Jun MATSUYAMA, Muneaki SHIGETA, Taichi TAKEZAKI, Toru SASAKI[1)] and Hiroaki ITO

Faculty of Engineering, University of Toyama, 3190 Gofuku, Toyama 930-8555, Japan
[1)]*Department of Science of Technology Innovation, Nagaoka University of Technology, 1603-1 Kamitomioka, Nagaoka, Niigata 940-2188, Japan*

(Received 6 January 2023 / Accepted 25 April 2023)

To understand the mechanism of particle acceleration in collisionless shocks, generating a collisionless plasma flowing through dilute gas is required. We have proposed a compact plasma focus (CPF) device to generate collisionless plasma by using pulsed-power discharge. To discuss a particle acceleration process in collisionless shocks, it is necessary to evaluate an ion energy distribution function (IEDF) of the plasma. In this study, we measured the IEDF of the plasma flow using a retarding field energy analyzer (RFA). The experimental results measured by the RFA showed that ions with a few eV are dominant in the plasma flow generated by the CPF device. The IEDF could be fitted with the shifted Maxwellian distribution. The plasma parameters were estimated to be the ion number density $n_\mathrm{i} = 4.6^{+0.2}_{-0.8} \times 10^{19}$ m^{-3}, the ion temperature $T_\mathrm{i} = 0.8^{+0.6}_{-0.4}$ eV, and the drift velocity $v_\mathrm{d} = 11^{+0.5}_{-3.5}$ km/s. The estimated velocity approximately agreed with the result of a time-of-flight method calculated by the ion current waveform.

Keywords: collisionless shock, fast plasma flow, pulsed-power discharge, plasma focus, ion current measurement

DOI: 10.1585/pfr.18.2401049

1. Introduction

Understanding how to generate high-energy particles in outer space, called cosmic rays (CRs), is one of the important issues in astrophysics. The CRs are characterized by a maximum energy of 10^{20} eV and a non-thermal power-law energy spectrum [1, 2]. Collisionless shocks are considered one of CRs generator. Collisionless shocks are shock phenomena generated by the interaction of collisionless plasma and electromagnetic fields, such as shock around supernova remnants. Unlike hydrodynamical shocks on the earth, the energy dissipation process in collisionless shocks occurs through electromagnetic fields, and particle acceleration occurs in the process. However, the detailed generation mechanism of particle acceleration is not fully understood [3]. One method for understanding the mechanism of collisionless shocks is reproducing the shock in a laboratory-scale experiment and evaluating the phenomena in-site [4]. Requirements for reproducing collisionless shock in the laboratory-scale experiment have been proposed [5–7]. An important condition is the generation of a fast plasma flow in a dilute gas. Recently, collisionless shock experiments using high-power lasers have been conducted [8,9]. Although laser experiments can generate well-defined high-energy-density plasma, the experiments have issues with low shot-rates. We propose the generation of a collisionless plasma by pulsed-power discharge using a plasma focus (PF) device. The PF device is a technique for generating high-energy-density plasma and has been applied as ion and neutron beam sources [10–12]. The generation of the fast plasma flow using the PF device has a longer space-time scale and is easier to observe than high-power laser experiments. In addition, the pulsed-power experiment has high shot-rates. A tapered cone plasma focus device (TCPFD) produces a quasi-one-dimensional plasma flow with a drift velocity of $U \sim 30$ km/s, an ion number density $n_\mathrm{i} \sim 10^{20}$ m^{-3}, and an electron temperature $T_\mathrm{e} \sim 3$ eV in helium gas at 0.3 Pa [13–15]. To generate collisionless plasma, driving the PF device in dilute gas is required, different from typical PF devices. As a result, as the mean free path of particles would be long, typical MHD models inside PF devices can not be applied, and the plasma behavior inside the PF electrodes is unclear. Therefore, we have developed a compact PF (CPF) device with six columnar outer electrodes and an inner cone electrode to observe the plasma behavior inside the electrodes. Understanding the plasma parameters generated by the CPF device is required to discuss the particle acceleration mechanism in collisionless

author's e-mail: m2171012@ems.u-toyama.ac.jp, takezaki@eng.u- toyama. ac.jp

*) This article is based on the presentation at the 31st International Toki Conference on Plasma and Fusion Research (ITC31).

shock. In this study, we evaluate the ion energy distribution function (IEDF) of the fast plasma flow produced by the CPF device using a retarding field analyzer (RFA). We have measured ion current density using the RFA to understand the plasma parameters of the CPF device.

2. Experimental Setup

Figure 1 is a schematic image of the CPF device. The CPF device consists of anode electrodes, a cathode electrode, and an insulator. A pulsed-power discharge generates a plasma sheet at the surface of the insulator. The plasma sheet propagates in the direction of the tip of the cone electrode via a high current and a magnetic field induced by its current. At the tip of the cone electrode, the plasma sheet is compressed by a pinch effect, producing a thermal plasma. The inner cone electrode (cathode) had a height of 46 mm and diameter of 26 mm, and the six columnar outer electrodes (anode) had a height of 62 mm and inner angle of 76 deg. The vacuum chamber is filled with He gas at 0.5 Pa. The generated plasma flow is measured by the RFA located 25 mm from the top of the electrode.

Figure 2 is an equivalent circuit diagram of the CPF device. A discharge voltage is 12.5 kV, and the capacitor bank is 7.7 μF. The discharge current was measured by a Rogowski coil between a gap switch and the cathode electrode. The stray resistance and inductance of the CPF circuit, calculated from the discharge current waveform, were 30 mΩ and 65 nH, respectively.

Figure 3 is a configuration of the RFA. The RFA consists of an aperture to limit the flux, an electron reflection grid (ERG), an ion filter grid (IFG), and a collector to capture ions. The ERG and IFG grids are made of a stainless steel mesh (SUS304) with a wire diameter of 60 μm and an opening area of 0.01 mm^2. The collector is a Faraday cup for suppressing secondary electrons emission. The RFA is set up on a separate electrical ground from the CPF circuit to avoid noise via the discharge. Figure 4 shows the distribution of the applied voltage for each grid. The ERG was applied at −15 V for reflecting electrons. The IFG was swept from 0 to 15 V, and the collector was applied at −30 V to capture ions. The ion current density of ions captured by the collector is as follows:

$$J = \frac{V_{\text{out}}}{RS}, \tag{1}$$

where R is the termination resistance (50 Ω), V_{out} is the measured voltage, and S is the cross-section of the aperture

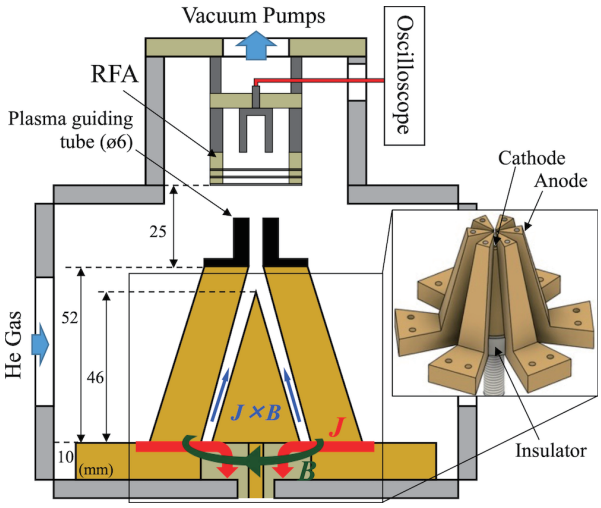

Fig. 1 Schematic image of the CPF device.

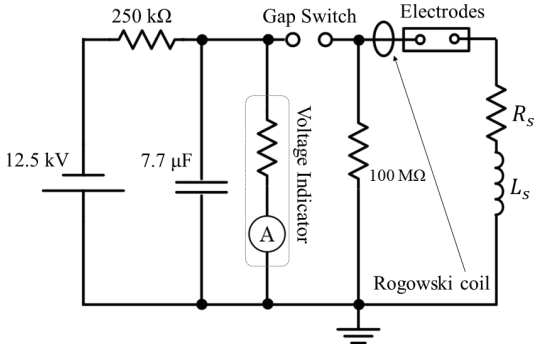

Fig. 2 Equivalent circuit diagram of the CPF device.

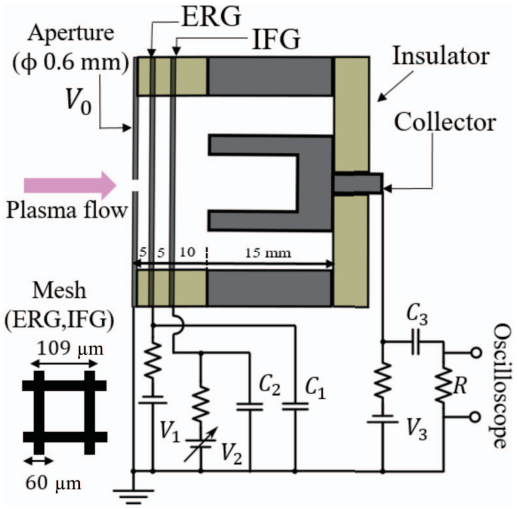

Fig. 3 Configuration of the RFA.

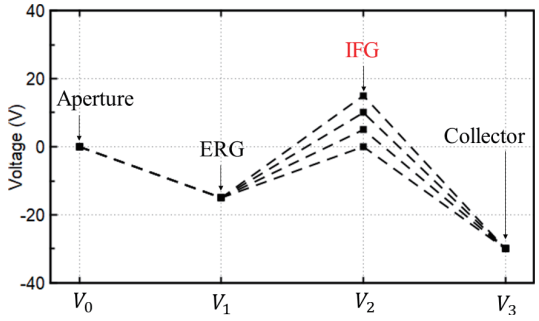

Fig. 4 Potential distribution of the RFA.

with the pinhole of ϕ0.6 mm.

3. Results and Discussion

3.1 Ion current density and drift velocity

Figure 5 shows typical waveforms of the discharge current and the ion current density at V_2 = 0, 5, and 15 V. As shown in Fig. 5 (a), the typical discharge current resulted in a decaying sine wave with a maximum current of 68 kA and a period of 7.5 µs. As shown in Figs. 5 (b) - (d), the ion current density waveforms measured by the RFA were evaluated by cutting off high frequencies considered noise. The ion current density decreased by increasing V_2. The increase in V_2 causes more ions to be reflected by the IFG, resulting in fewer ions reaching the collector and a decrease in ion current density. Comparing Figs. 5 (b) and 5 (c), the ion current density decreased significantly by increasing V_2 from 0 to 5 V. Thus, the plasma flow produced by the CPF device is dominated by the ion with energies of 0 - 5 eV. Comparing Figs. 5 (c) and 5 (d), the ion current density is less reduced by increasing V_2 from 5 to 15 V because the number of ions over 5 eV is small. The drift velocity of the plasma flow generated by the CPF device is calculated by a time-of-flight (TOF) method. The velocity is calculated from the peak time of the ion current and distance as follows:

$$U = \frac{d}{t_{\mathrm{peak}}}, \tag{2}$$

where d is the distance from the bottom of the cathode to the aperture of the RFA (71 mm), t_{peak} is the peak time of the ion current density. From Fig. 5 (b), the drift velocity was obtained as 12.7 km/s.

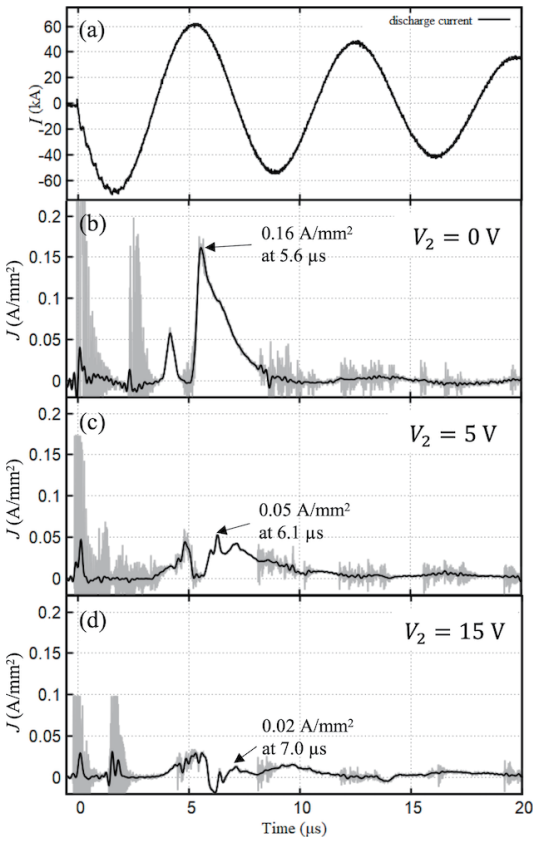

Fig. 5 Typical waveform of the discharge current and ion current density. (a) The discharge current. The ion current density at (b) V_2 = 0 V, (c) V_2 = 5 V, and (d) V_2 = 15 V.

3.2 Evaluation of IEDF as shifted Maxwellian

Plasma parameters were estimated from a V-I characteristic measured by the RFA. The ion current density measured at the collector of V_2 = 0 V is described as follows:

$$J_0 = eZn_{\mathrm{i}} \int_0^{\infty} v f_{\mathrm{i}}(v)\, dv, \tag{3}$$

where e is an elementary charge, Z is a charge state (assuming Z = 1), n_{i} is the ion number density, v is velocity of ions, and f_{i} is ion velocity distribution function. Because f_{i} assumes the shifted Maxwellian distribution, f_i can be expressed as follows:

$$f_{\mathrm{i}}(v)\, dv = \left(\frac{M}{2\pi k_{\mathrm{b}} T_{\mathrm{i}}}\right)^{\frac{1}{2}} \exp\left(-\frac{M|v - v_{\mathrm{d}}|^2}{2k_{\mathrm{b}} T_{\mathrm{i}}}\right) dv, \tag{4}$$

where M is helium ion mass, k_{b} is a Boltzmann constant, T_{i} is the ion temperature, and v_{d} is the drift velocity of the plasma flow. From $Mv^2/2 = eV_2 = E_2$, the relationship between the velocity and the energy can be expressed as follows:

$$dv = \frac{1}{Mv} dE_2. \tag{5}$$

From Eqs. (3) - (5), the ion current density dependence on E_2 is expressed as follows:

$$J(E_2) = J_0 - \frac{eZn_{\mathrm{i}}}{M} \int_0^{E_2} f_{\mathrm{i}}(E_2)\, dE_2. \tag{6}$$

Figure 6 shows the ion current density dependence on V_2, and the estimated IEDF assuming the shifted Maxwellian. As shown in Figs. 5 (b) - (d), the ion current waveforms measured by the RFA have two peaks. As

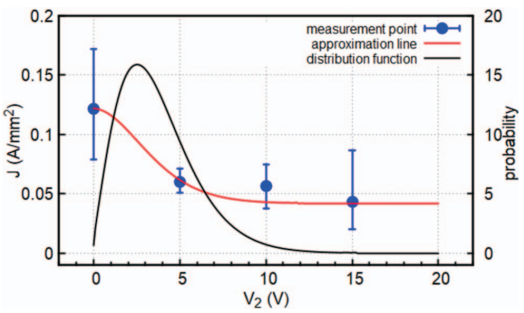

Fig. 6 V-I characteristic of the current density dependence on V_2. The values of the experimental results are averages of the five shots. The approximation line was fitted by $n_{\mathrm{i}} = 4.6 \times 10^{19}$ m^{-3}, T_{i} = 0.8 eV, and v_{d} = 11 km/s.

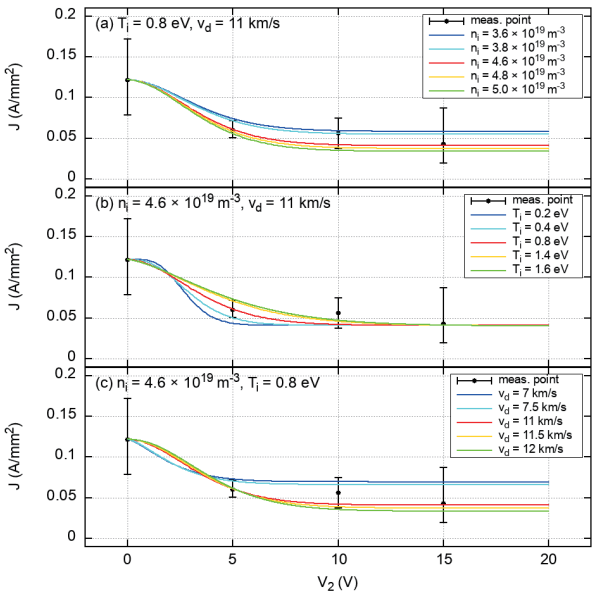

Fig. 7 Evaluation of the parameter ranges by changing (a) n_i, (b) T_i, and (c) v_d.

the first peak was present even with increasing V_2, it may be attributed to high-energy ions. However, the presence of high-energy ions is unclear because the plasma generation process and the dynamics inside the electrodes are not clarified in the CPF device. Therefore, we have evaluated the second peak as the main bulk of the plasma. The result indicates that the IEDF of the plasma flow generated by the CPF device can be fitted by the shifted Maxwellian as shown in Eq. (6) with the parameters of $n_i = 4.6 \times 10^{19}\,\mathrm{m}^{-3}$, $T_i = 0.8\,\mathrm{eV}$, and $v_d = 11\,\mathrm{km/s}$. The fitted IEDF was dominated by helium ions with energies of a few eV. The almost unchanged ion current density at $V_2 = 10$ - $15\,\mathrm{V}$ shown in Fig. 6 is explained because the population of the ions with energies of 10 - 15 eV is low. Moreover, the velocity was approximately equal to the drift velocity obtained by the TOF method. Figure 7 shows the evaluation of the parameter ranges of n_i, T_i, and v_d. By fitting the experimental error bars of the V-I characteristic, the plasma parameters are estimated to be $n_i = 4.6^{+0.2}_{-0.8} \times 10^{19}\,\mathrm{m}^{-3}$, $T_i = 0.8^{+0.6}_{-0.4}\,\mathrm{eV}$, and $v_d = 11^{+0.5}_{-3.5}\,\mathrm{km/s}$.

4. Conclusion

We measured the ion current density and the drift velocity of the plasma flow generated by the CPF device using the RFA. The RFA results showed that the ion current density changed with the IFG voltage V_2. Increasing V_2 from 0 to 5 V decreased the ion current density significantly. The result indicates that the plasma generated by the CPF device consists of ions of a few eV. Moreover, the plasma flow velocity generated by the CPF device was estimated to be 12.7 km/s using the TOF method with the ion current density waveform. The V-I characteristic measured by the RFA could be fitted with the shifted Maxwellian. The plasma parameters of the ion number density $n_i = 4.6^{+0.2}_{-0.8} \times 10^{19}\,\mathrm{m}^{-3}$, the ion temperature $T_i = 0.8^{+0.6}_{-0.4}\,\mathrm{eV}$, and the drift velocity $v_d = 11^{+0.5}_{-3.5}\,\mathrm{km/s}$ were obtained. The velocity calculated from the TOF method and the velocity obtained by fitting to the shifted Maxwellian is approximately the same.

In the future, we will evaluate the plasma dynamics inside the electrodes. Moreover, we will apply a magnetic field to the plasma flow and evaluate the change of the IEDF of the plasma flow in the magnetic field.

Acknowledgments

This work was partly supported by JSPS KAKENHI Grant No. 20K14440, and 23K13079.

[1] S. Swordy, in *The Astrophysics of Galactic Cosmic Rays* (Springer, 2001), pp. 85-94.
[2] J. Linsley, Phys. Rev. Lett. **10**, 146 (1963).
[3] A.R. Bell, Mon. Not. R. Astron. Soc. **182**, 147 (1978).
[4] T. Ide, Y. Sakawa, Y. Kuramitsu, T. Morita, H. Tanji, K. Nishio, M. Kuwada, H. Ide, K. Tsubouchi, S. Shimazaki *et al.*, EPJ Web of Conferences **59**, 15002 (2013).
[5] R. Drake, Phys. Plasmas **7**, 4690 (2000).
[6] D. Ryutov, B. Remington, H. Robey and R. Drake, Phys. Plasmas **8**, 1804 (2001).
[7] A. Stockem, F. Fiuza, A. Bret, R. Fonseca and L. Silva, Sci. Rep. **4**, 3934 (2014).
[8] R. Yamazaki, S. Matsukiyo, T. Morita, S.J. Tanaka, T. Umeda, K. Aihara, M. Edamoto, S. Egashira, R. Hatsuyama, T. Higuchi *et al.*, Phys. Rev. E **105**, 025203 (2022).
[9] D. Schaeffer, W. Fox, D. Haberberger, G. Fiksel, A. Bhattacharjee, D. Barnak, S. Hu and K. Germaschewski, Phys. Rev. Lett. **119**, 025001 (2017).
[10] K. Kondo, M. Nakajima, T. Kawamura and K. Horioka, Rev. Sci. Instrum. **77**, 036104 (2006).
[11] V.A. Gribkov, A. Banaszak, B. Bienkowska, A.V. Dubrovsky, I. Ivanova-Stanik, L. Jakubowski, L. Karpinski, R.A. Miklaszewski, M. Paduch, M.J. Sadowski *et al.*, J. Phys. D: Appl. Phys. **40**, 3592 (2007).
[12] M. Sohrabi, Z. Soltani and M. Habibi, Radiat. Phys. Chem. **172**, 108836 (2020).
[13] T. Sasaki, H. Kinase, T. Takezaki, K. Takahashi, T. Kikuchi, T. Aso and N. Harada, JPS Conf. Proc. **1**, 015096 (2014).
[14] T. Takezaki, S. Kato, T. Oguchi, S. Watanabe, K. Takahashi, T. Sasaki, T. Kikuchi and H. Ito, Phys. Plasmas **28**, 102109 (2021).
[15] T. Takezaki, K. Takahashi, T. Sasaki, T. Kikuchi and N. Harada, Phys. Plasmas **23**, 062904 (2016).